Interaction of Surfactin with Membranes: A Computational Approach

Magali Deleu,*,† Olivier Bouffioux,‡ Hary Razafindralambo,† Michel Paquot,† Choukri Hbid,§ Philippe Thonart,§ Philippe Jacques,|| and Robert Brasseur‡

Unité de Chimie Biologique Industrielle, Centre de Biophysique Moléculaire Numérique, Unité de Bio-Industries, Faculté Universitaire des Sciences Agronomiques de Gembloux, 2 Passage des Déportés, B-5030 Gembloux, Belgium; and Centre Wallon de Biologie Industrielle, Sart-Tilman, 4000 Liège, Belgium

Received September 12, 2002. In Final Form: January 30, 2003

Modeling analysis was used to understand the molecular mechanisms of the biological activities of surfactin, in particular, its hemolytic activity. This study highlights the importance of the fatty acid chain hydrophobicity of the surfactin on its activities, the C15 homologue being the most active. This is related to its self-association capacity. The detergent effect is the predominant mechanism involved in the hemolytic activity. A two-step mechanism is suggested, depending on the surfactin concentration. Other mechanisms (cationic channel, mobile carrier) can also be involved in particular conditions.

Introduction

Surfactin is a lipopeptide excreted by different strains of *Bacillus subtilis*. It is a cyclic heptapeptide closed by a β-hydroxy fatty acid chain.[1] It is an attractive compound thanks to its powerful surface and interface activity.[2−5] In addition, it exhibits many interesting bioactive properties, including antiviral, antimycoplasma, antibacterial, and hemolytic activities.[6−8]

The biological activity of surfactin results from the interaction of the molecule with the membrane of target cells. However, the detailed molecular mechanism of action is not clearly understood. Different suggestions have been reported in the literature.

Sheppard et al.[9] have shown that surfactin induces cationic channels in planar lipid bilayers, leading to permeability changes. They have suggested an interaction between surfactin and ions in the aqueous phase followed by a partitioning into the membrane, and the formation of channels.

According to Thimon et al.,[10] surfactin is also a mobile carrier, which transports monovalent and divalent cations across the membrane, leading to perturbation of osmotic equilibrium. They have suggested that the complexation of cations by surfactin takes place at the interface, the complex being then solubilized in the lipid phase.

Others[7,8] have assumed that surfactin interacts with the lipid bilayer, leading, at high concentrations, to membrane disruption by a detergent effect. Heerklotz and Seelig[11] have also suggested a detergent-like action on the basis of isothermal titration calorimetry experiments.

According to Epand,[12] lipopeptides should modify the bulk physical properties of membranes, leading to an alteration of membrane functions such as fusion and the activity of membrane-bound enzymes. In the case of iturin A, another lipopeptide produced by *B. subtilis*, Grau et al.[13] have shown that its insertion in the bilayer modifies the membrane curvature.

The composition of the phospholipid bilayer influences the penetration of surfactin.[14] Ionized surfactin (with two negative charges) inserts deeper in L-α-dimyristoyl phosphatidylcholine (DMPC) than in L-α-dimyristoyl phosphatidylethanolamine (DMPE) monolayers. The insertion is greatly reduced in L-α-dimyristoyl phosphatidic acid (DMPA) monolayers because of electrostatic repulsions. The surfactin penetration is also lowered when the length of phospholipid acyl chains increases.

According to Kracht et al.,[15] the inactivation of enveloped viruses by surfactin depends on its hydrophobicity, that is, on the number of carbon atoms of its fatty acid chain and on the charge of its peptide moiety. A high number of carbon atoms (C15) in the fatty acid chain and a single negative charge in the peptide ring result in more active compounds.

The mechanisms described in the literature (channel formation, mobile carrier, detergent effect) are based on

* Corresponding author. Phone: (+32) 81 62 22 32. Fax: (+32) 81 62 22 31. E-mail: deleu.m@fsagx.ac.be.
† Unité de Chimie Biologique Industrielle.
‡ Centre de Biophysique Moléculaire Numérique.
§ Centre Wallon de Biologie Industrielle.
|| Unité de Bio-Industries.

(1) Kakinuma, A.; Ouchida, A.; Shima, T.; Sugino, H.; Isono, M.; Tamura, G.; Arima, K. *Agric. Biol. Chem.* **1969**, *33*, 1669−1671.
(2) Maget-Dana, R.; Ptak, M. *J. Colloid Interface Sci.* **1992**, *1*, 285−291.
(3) Razafindralambo, H.; Popineau, Y.; Deleu, M.; Hbid, C.; Jacques, P.; Thonart, P.; Paquot, M. *J. Agric. Food Chem.* **1998**, *46*, 911−916.
(4) Deleu, M.; Razafindralambo, H.; Popineau, Y.; Jacques, P.; Thonart, P.; Paquot, M. *Colloids Surf., A* **1999**, *152*, 3−10.
(5) Deleu, M.; Paquot, M.; Razafindralambo, H.; Popineau, Y.; Budziekiewicz, H.; Jacques, P.; Thonart, P. In *Food emulsions and foams: Interfaces, Interactions and Stability*; Dickinson, E., Rodríguez Patino, J. M., Eds.; Royal Society of Chemistry: London, Cambridge, 1999; pp 296−304.
(6) Bernheimer, A. W.; Avigad, L. S. *J. Gen. Microbiol.* **1970**, *61*, 361−369.
(7) Vollenbroich, D.; Pauli, G.; Özel, M.; Vater, J. *Appl. Environ. Microbiol.* **1997**, *63*, 44−49.
(8) Vollenbroich, D.; Özel, M.; Vater, J.; Kamp, R. M.; Pauli, G. *Biologicals* **1997**, *25*, 289−297.
(9) Sheppard, J. D.; Jumaric, D. G.; Copper, D. G.; Laprade, R. *Biochim. Biophys. Acta* **1991**, *1064*, 12−23.
(10) Thimon, L.; Peypoux, F.; Wallach, J.; Michel, G. *Colloids Surf., B* **1993**, *1*, 57−62.
(11) Heerklotz, H.; Seelig, J. *Biophys. J.* **2001**, *81*, 1547−1554.
(12) Epand, R. M. *Biopolymers* **1997**, *43*, 15−24.
(13) Grau, A.; Gomez-Fernandez, J. C.; Peypoux, F.; Ortiz, A. *Peptides* **2001**, *22*, 1−5.
(14) Maget-Dana, R.; Ptak, M. *Biophys. J.* **1995**, *66*, 1937−1943.
(15) Kracht, M.; Rokos, H.; Özel, M.; Kowall, M.; Pauli, G.; Vater, J. *J. Antibiot.* **1999**, *52*, 613−619.

10.1021/la026543z CCC: $25.00
Published on Web 03/08/2003

different unrelated experiments. No critical review of these different mechanisms has yet been published. In this paper we propose to use computational methods to gain a better insight, at the molecular level, of the various mechanisms.

The channel formation and the mobile carrier hypotheses were studied by use of the IMPALA procedure.[16] In this method a simple restraint field accounts for the membrane properties and the insertion of a single molecule is analyzed by a Monte Carlo procedure applied to restraint functions.

The results obtained with IMPALA led us to investigate the detergent effect mechanism. HYPERMATRIX[17] was used to study the propensity of surfactin to interact with itself and with phospholipid molecules. HYPERMATRIX was used to assemble one central molecule with other surrounding molecules at an air/water interface. HYPERMATRIX has been successfully used to compute peptide−lipid,[18] pharmacological drug−lipid,[19] and protein−lipid[20] assemblies.

The two methods, with their advantages and limitations, lead to valuable information about the action mechanisms of surfactin in biological membranes, more specifically about its hemolytic activity.

Theoretical Calculations

IMPALA Simulations. IMPALA uses a membrane model in which the phospholipid molecules are implicitly modeled by an empirical function $C(z)$ and the membrane properties are modeled by energetic restraints.[21] This model takes into consideration the general properties of membranes and has already been successfully applied to the study of peptides[22] and protein penetration[23,24] in bilayers.

Description of the Bilayer Model. Assuming that the properties of a membrane are constant in the plane of the bilayer, the lipid/water interfaces are described by an empirical function, $C(z)$, which varies along the z axis only. z (in Å) is perpendicular to the plane of the membrane, and its origin is at the bilayer center.

$C(z)$ (Figure 1) varies from 1 (completely hydrophilic) to 0 (completely hydrophobic). It is derived from ref 25:

$$C(z) = 1 - \frac{1}{1 + e^{\alpha(|z|-z_0)}} \qquad (1)$$

where α and z_0 are parameters calculated so that $C(|z = 18\text{Å}|) = 1$ and $C(|z = 13.5\ \text{Å}|) = 0$. $C(z)$ is approximately constant from $-\infty$ to -18 Å (hydrophilic phase), from -13.5 Å to 13.5 Å (hydrocarbon core), and from 18 Å to ∞ (hydrophilic phase). $z = 0$ Å is the membrane center, $z = \pm 13.5$ Å is the distance where the first polar heads of lipids appear, and $z = \pm 18$ Å is the distance beyond which there is only water. The same interface width was used in the Monte Carlo technique developed by Milik and Skolnick.[25]

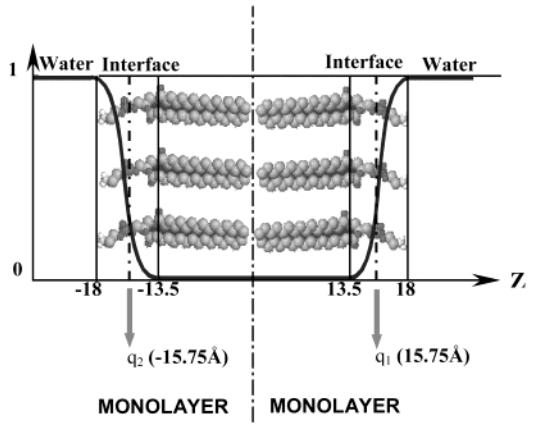

Figure 1. Evolution of the $C(z)$ function in the bilayer membrane as applied in the IMPALA procedure. The gray phospholipids are shown to better visualize interface location in the bilayer model. They are not explicitly taken into account in simulations.

Description of the Energetic Restraints. The total energetic restraint computed during the simulations results from three components:

(1) Hydrophobic Restraint. Water compels the hydrophobic atoms to penetrate within the hydrophobic core of the bilayer. The segregation of hydrophobic and hydrophilic parts of the molecule imposed by the membrane properties is known as the hydrophobic effect. This is simulated by the hydrophobic restraint E_{int}:

$$E_{\text{int}} = -\sum_{i=1}^{n} S_{(i)} E_{\text{tr}(i)} C_{(z_i)} \qquad (2)$$

where $S_{(i)}$ is the accessible surface of atom i among the n atoms of the molecule, $E_{\text{tr}(i)}$ is its transfer energy in units of accessible surface area, and $C(z_i)$ is the value of $C(z)$ at the position z_i of atom i.

This restraint increases when hydrophilic atoms penetrate into the membrane model and decreases when hydrophobic atoms do. The most accessible are the atoms, the largest is the effect.

(2) Lipid Perturbation Restraint. The structure of a biological membrane is stabilized by interactions between lipids. When a molecule penetrates into the membrane, interactions between adjacent lipids are disrupted and replaced by molecule−lipid ones. Thus, lipids are opposing the insertion of any molecule. This effect is simulated with the lipid perturbation restraint E_{lip}:

$$E_{\text{lip}} = a_{\text{lip}} \sum_{i=1}^{n} S_{(i)} C(z_i) \qquad (3)$$

where $a_{\text{lip}} = 0.018$ is an empirical parameter, $S_{(i)}$ is the accessible surface of atom i, and $C(z_i)$ is the value of C at the position z_i of the atom. E_{lip} increases with the surface of the molecule in contact with lipids.

(3) Charge Restraint. This restraint reflects the charged/uncharged phospholipid balance in a biological membrane, as shown by Cullis et al.,[26] by using a surface charge

(16) Ducarme, Ph.; Rahman, M.; Brasseur, R. *Proteins: Struct., Funct., Genet.* **1998**, *30*, 357−371.
(17) Brasseur, R. In *Molecular Description of Biological membranes by Computer Aided Conformational Analysis*; Brasseur, R., Ed.; CRC Press: Boca Raton, FL, 1990; Vol. 1, pp 203−219.
(18) Brasseur, R.; Cabiaux, V.; Killian, J. A.; de Kruijff, B.; Ruysschaert, J. M. *Biochim. Biophys. Acta* **1986**, *855*, 317−324.
(19) Mingeot-Leclercq, M. P.; Gallet, X.; Flore, C.; Van Bambeke, F. *Antimicrob. Agents Chemother.* **2001**, *45*, 3347−3354.
(20) Lins, L.; Flore, C.; Chapelle, L.; Talmud, P. J.; Thomas, A.; Brasseur, R. *Protein Eng.* **2002**, *15*, 513−520.
(21) Bouffioux, O.; Basyn, F.; Rezsohazy, R.; Brasseur, R. In *Cell-penetrating peptides − Processes and applications*; Langel, U., Ed.; CRC Press: Boca Raton, London, New York, Washington, 2002; pp 187−222.
(22) Lins, L.; Charloteaux, B.; Thomas, A.; Brasseur, R. *Proteins: Sruct., Funct., Genet.* **2001**, *44*, 435−447.
(23) Basyn, F.; Charloteaux, B.; Thomas, A.; Brasseur, R. *J. Mol. Graphics Modell.* **2001**, *20*, 235−244.
(24) Basyn, F.; et al. *J. Mol. Graphics Modell.*, submitted.
(25) Milik, M.; Skolnick, J. *Proteins* **1993**, *15*, 10−25.
(26) Cullis, P. R.; Fenske, D. B.; Hope, M. J. In *Biochemistry of Lipids, Lipoproteins and Membranes*; Vance, D. E., Vance, J., Eds.; Elsevier: North-Holland, Amsterdam, 1996; Vol. 31, pp 1−33.

density. We use 0.005 $e^-/Å^2$ for the inner leaflet of our model in order to mimic the human erythrocyte membrane.[26]

The surface charge density is localized in a plane, parallel to the bilayer, at +15.75 Å and/or −15.75 Å from the bilayer center.

The charge restraint E_q is calculated as follows:

$$E_q = \sum_i^n q_i \frac{2k\pi\delta}{\epsilon(z)} \tag{4}$$

where q_i is the atomic charge of atom i, δ is the superficial charge density attributed to the plane, and k is a constant. The model of the dielectric profile along the bilayer normal, $\epsilon(z)$, is from Flewelling and Hubbel:[24]

$$\epsilon(z) = \epsilon_{\text{pho}} + (\epsilon_{\text{phi}} - \epsilon_{\text{pho}})[1 + 10^{4(d+z)/h}]^{-1} \tag{5}$$

where $\epsilon_{\text{pho}} = 2$ is the value of the dielectric constant in the hydrophobic core of the membrane and $\epsilon_{\text{phi}} = 78$ is the value in bulk water. This function provides a smooth transition in the interfacial region, that is defined by two parameters, d and h, the center and width of the transition region, respectively.

Monte Carlo Procedure. The best position and orientation of a molecule interacting with the membrane model are calculated using a standard Monte Carlo procedure of 3×10^5 steps at 310 K with random displacements of maximum 2 Å/step and rotations of maximum 2°/step of the molecule in order to find the lowest total energetic restraint. Since the inserted molecule is rigid during the analysis, its intramolecular energy is constant and the restraints described above are the only energy terms taken into account for the minimization.

The molecule starts the Monte Carlo procedure randomly oriented with its mass center at +30 Å from the bilayer center. Each procedure was run three times.

HYPERMATRIX Procedure. The procedure originally used to surround one molecule with phospholipids[17] is summarized as follows (Figure 2):

Surfactin−Lipid Complex. (A) The surfactin position was fixed and the lipid position was moved along the *x*-axis by steps of 0.3 Å. (B) At each step, the lipid molecule was rotated 12 times around its long axis and around the surfactin *z*-axis. (C) The lipid was allowed to move along the *z*-axis perpendicular to the interface. (D) Finally, the tilt of the lipid molecule was varied with respect to the *z*-axis. The energy of all possible positions is calculated; only the complex of minimum energy is kept.

Then, the position of the first lipid was fixed and the addition of a second lipid molecule was considered. The energies of interaction between all molecules of the complex are considered and minimized until the lowest energy structure is reached.

The same method was used to assemble a central surfactin molecule with other surrounding surfactin molecules.

The intermolecular energy of interaction in the complex is calculated as the sum of the following terms: (a) The London−van der Waals energy of interaction between atoms associated to different molecules. Buckingham's pairwise atom−atom interaction function has been used:

$$E_{\text{vdW}} = \sum_{ij}[A_{ij} \exp(-B_{ij} r_{ij}) - C_{ij} {r_{ij}}^{-6}] \tag{6}$$

where i and j are atoms, r_{ij} are their distances, and A, B, and C are coefficients assigned to atom pairs. We used the values of the coefficients reported by Liquori and coworkers.[25,26] These values emerge in part as the solution of the Schrödinger equation and in part as heuristic variables. The problem in this potential is that if the atoms were to approach less than about 1 Å from one another, the r^{-6} attractive term becomes dominant, causing the total energy of the molecule to collapse to negative infinity. This is why an energy (E_{vdW}) of 100 kcal/mol is substituted for distances (r_{ij}) below 1 Å.

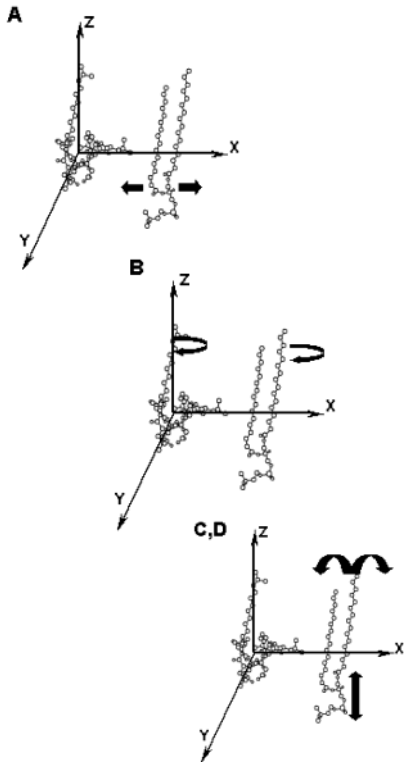

Figure 2. HYPERMATRIX assembly procedure used to surround one surfactin molecule with other surfactin molecules or with phospholipid molecules. See text (Experimental Methods) for details.

(b) The generalized Keesom-−van der Waals interaction or electrostatic interaction between atomic point charges:

$$E_{cb} = 332\left(\sum_{ij} \frac{e_i e_j}{r_{ij}\epsilon}\right) \tag{7}$$

where e_i and e_j are expressed in electron charge units and r_{ij} is in Å. The values of the atomic point charges are similar to the values used for polypeptides.[30] To simulate the electrostatic properties of the membrane interface, we have assumed a dielectric constant (ϵ) equal to 3 in the hydrophobic core and 30 in the water phase. Between these two media, there is an interface where the dielectric constant increases linearly along the *z*-axis perpendicular to the interface.

(c) The transfer energy of atoms or groups of atoms from a hydrophobic phase to a hydrophilic phase.[31]

(27) Flewelling, R. F.; Hubbel, W. L. *Biophys. J.* **1986**, *49*, 541−552.
(28) Liquori, A. M.; Giglio, E.; Mazzarella, L. *Nuovo Cimento.* **1968**, *55B*, 475−480.
(29) Giglio, E.; Liquori, A. M.; Mazzarella, L. *Nuovo Cimento* **1968**, *56*, 57−62.
(30) Hopfinger, A. J. In *Conformational Properties of Macromolecules*; Academic Press: New York, 1973.
(31) Tanford, C. In *The Hydrophobic Effect. Formation of Micelles and Biological Membranes*; Tanford, C., Ed.; Wiley: New York, 1973.

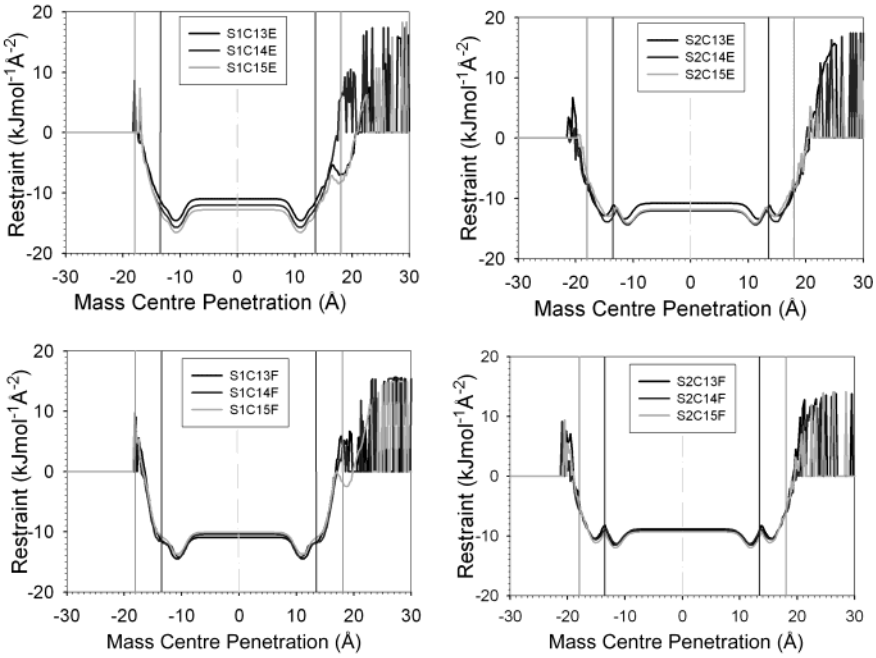

Figure 3. Evolution of the total restraint as a function of the molecule mass center penetration in an uncharged bilayer. The vertical lines correspond (from left to right) to the plane between the bilayer and the aqueous phase ($z = \pm 18$ Å), the plane between the hydrocarbon core and the hydrophilic head of the bilayer ($z = \pm 13.5$ Å), and the center of the bilayer ($z = 0$ Å). At the beginning of the procedure, the molecule mass center was in the aqueous phase (+30 Å).

Table 1. List of the Surfactin Molecules Analyzed by the IMPALA Procedure

extended chain (E)		folded chain (F)	
S1 ring	S2 ring	S1 ring	S2 ring
S1C13E	S2C13E	S1C13F	S2C13F
S1C14E	S2C14E	S1C14F	S2C14F
S1C15E	S2C15E	S1C15F	S2C15F

Experimental Methods

Hemolytic Activity. The measurement of the hemolytic activity was carried out using synthetic plasma, as described by Yee-Hsiung et al.[32]

A sheep erythrocytes suspension (Diagnostic Pasteur) was diluted in 0.15 M NaCl to obtain 5×10^8 cells/mL.

The chemical composition of the synthetic plasma (mM) was 6.4 Arg·HCl, 22.6 Gly, 6.9 His·HCl hydrated, 6.9 Ile, 15.6 Leu, 16.9 Lys·HCl dihydrated, 8 Met, 8.8 Phe, 7.6 Thr, 1.5 Trp, 8.6 Val, 0.857 dextran T70, and 274 D-sorbitol. All chemicals were analysis-grade. Milli Q water was used. The pH of the solution was 8.

The production and extraction of the surfactin homologues were carried out as detailed in ref 3. Purified surfactin homologues were dissolved in 20 μL of a 0.2 M Tris buffer at pH 8. 880 μL of the synthetic plasma solution and 100 μL of the erythrocyte solution were successively added. The mixture was vortexed before incubation at 37 °C for 1 h.

Hemolysis was assayed spectroscopically. The hemolysis percentage (%) was estimated from the equation

$$H\% = 100(A_{int} - A_{obs})/(A_{int} - A_{lys}) \quad (8)$$

where A_{int} and A_{lys} are the absorbances at 540 nm of intact and lysed erythrocytes, respectively, and A_{obs} is the absorbance measured in the presence of surfactin. A_{lys} was obtained by a 1/10 dilution in distilled water. A_{int} was obtained by adding 100 μL of the erythrocyte solution and 880 μL of the synthetic plasma solution to 20 μL of Tris buffer without surfactin. Each experiment was performed at least twice.

Critical Micelle Concentration (cmc). The critical micelle concentration of the surfactin homologues in a Tris HCl pH 8.0 buffer at 20.0 °C was determined from the equilibrium surface tension versus surfactin concentration plots. The equilibrium

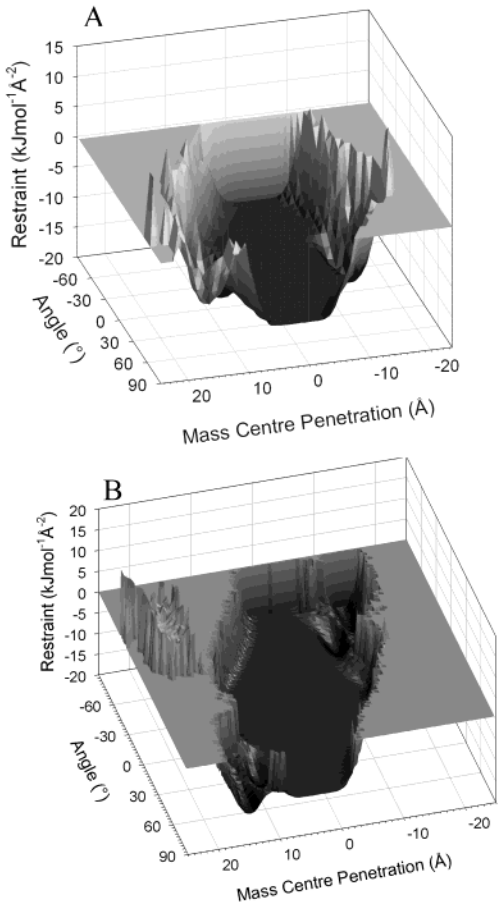

Figure 4. Evolution of the total restraint as a function of the molecule mass center penetration and the angle between the fatty acid chain and the plane of the bilayer for an uncharged bilayer: A, S1C15E; B, S2C15E. The IMPALA simulation started at the +30 Å mass center position.

(32) Yee-Hsiung, C.; Chien-Tsung, H.; Tsi, J. Y. *Biochem. Int.* **1984**, *8*, 329−338.

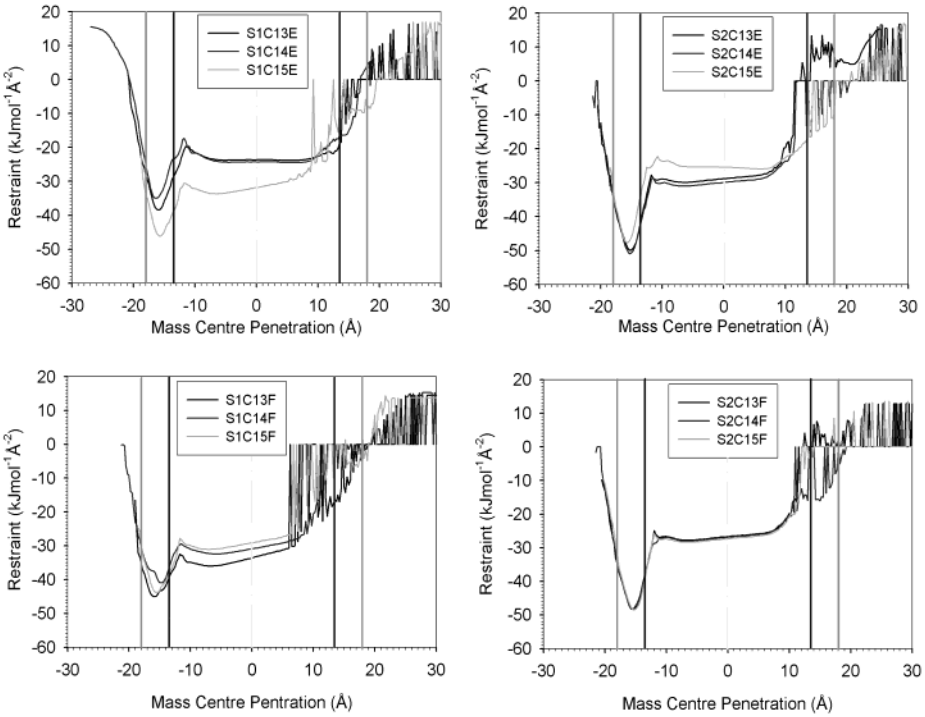

Figure 5. Evolution of the total restraint as a function of the molecule mass center penetration in a bilayer with a superficial charge density of 0.005 $e^-/Å^2$ in the inner sheet. See Figure 2 for the vertical lines legend. The simulation has begun at the +30 Å mass center position.

surface tension was measured as with the automated drop volume tensiometer TVT1 (Lauda-Königshofen, Germany) in the quasi-static mode. This method has been shown to provide accurate results, as obtained with the Wilhelmy's plate method.[33] All assays were performed twice.

Results

Simulation of the Surfactin Insertion in an Uncharged and a Charged Bilayer. The surfactin molecules were modeled in a previous paper.[34] Two peptide ring conformers (S1 and S2) were investigated on the basis of NMR analysis.[35] On each conformer, three different fatty acid chains were added (C13, C14, and C15) and were submitted to an energy minimization. Two structures (a folded and an extended) were obtained for each of them. Twelve molecules (Table 1) were then analyzed with IMPALA.

For each molecule in the uncharged bilayer, the profile of the total restraint is symmetric with respect to the center of the bilayer (Figure 3). This reflects the symmetrical properties of the bilayer model.

The restraint reaches a minimal value when the molecule mass center is located near the hydrophobic tails/polar heads interface of either bilayer sheet (about +11 or −11 Å). In the hydrocarbon core of the membrane, the restraint is constant and slightly higher than the minimum values. It increases drastically when the molecule leaves the bilayer.

There is little difference between the three homologues with respect to the peptide ring conformation and the fatty acid chain structure.

For a given fatty acid chain hydrophobicity (C13 or C14 or C15), differences in the peptide ring conformation and the fatty acid chain structure (folded or extended) do not exert a pronounced influence on the restraint profile. However, the minimum restraint is slightly lower for S1 conformers (between −16.5 and −13.7 kJ mol^{-1} $Å^{-2}$) than for S2 ones (between −14.4 and −11.3 kJ mol^{-1} $Å^{-2}$). The extended form of the fatty acid chain has also a slightly lower minimum restraint (between −16.5 and −13.4 kJ mol^{-1} $Å^{-2}$) than the folded one (between −14.5 and −11.3 kJ mol^{-1} $Å^{-2}$).

In the case of the extended fatty acid chains, the evolution of the restraint as a function of both the mass center penetration and the angle between the fatty acid chain and the plane of the bilayer was observed (Figure 4).

Only the C15 homologue is presented, since the results for the two others are similar. When the molecule penetrates into the bilayer, the extended fatty acid chain of the S1 and S2 conformers forms an angle of about 0° and 55° with the plane of the bilayer, respectively. In the hydrophobic core of the membrane (between +10 and −10 Å), the angle can vary in a wide range without affecting the restraint. On the other side of the hydrophobic core, the orientation of surfactin is inversed with negative values of angles (0° and −55°) for S1 and S2 conformers, respectively.

The profile of the total energy restraint is partially modified when the inner sheet of the bilayer has a surface charge density (0.005 $e^-/Å^2$) in order to mimic the human erythrocyte membrane[23] (Figure 5).

Unlike the case of the uncharged bilayer model, the total restraint in the charged bilayer decreases sharply toward a minimal value (about −45 kJ mol^{-1} $Å^{-2}$) when the mass center is in the polar head region of the inner sheet (between −13.5 and 18.0 Å). The minimal energy restraint is 3-fold lower in this case.

The S2 structures reach a lower restraint minimal value (between −48 and −50 kJ mol^{-1} $Å^{-2}$) than the S1 conformers (between −34 and −45 kJ mol^{-1} $Å^{-2}$).

(33) Razafindralambo, H.; Blecker, C.; Delhaye, S.; Paquot, M. *J. Colloid Interface Sci.* **1995**, *174*, 373−377.
(34) Gallet, X.; Deleu, M.; Razafindralambo, H.; Jacques, P.; Thonart, P.; Paquot, M.; Brasseur, R. *Langmuir* **1999**, *15*, 2409−2413.
(35) Bonmatin, J. M.; Genest, M.; Labbé, H.; Ptak, M. *Biopolymers* **1994**, *37*, 975−986.

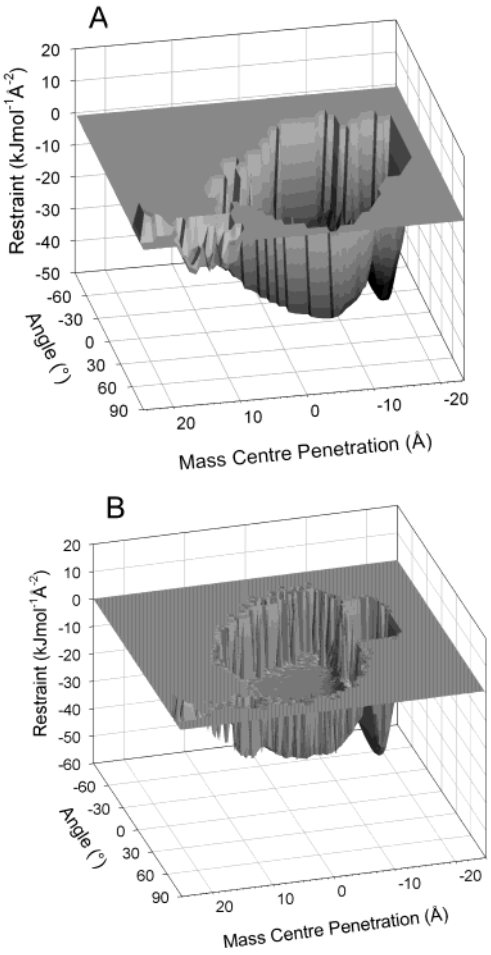

Figure 6. Evolution of the total restraint as a function of both the molecule mass center penetration and the angle between the fatty acid chain and the plane of the bilayer for a bilayer with a charge density of 0.005 $e^-/Å^2$ in the inner sheet: A, S1C15E; B, S2C15E.

An influence of the fatty acid chain hydrophobicity is observed for the S1 extended surfactins: the restraint is lower for the C15 homologue than for the C13 and C14 molecules. Nevertheless, the differences between the two peptide ring conformations, and the fatty acid chain forms are not obvious.

The 3D plot of the total restraint evolution as a function of both the mass center position and the angle between the fatty acid chain and the plane of the bilayer is also modified by the presence of charges in the inner sheet of the bilayer (Figure 6).

The surfactin molecule penetrates in the polar head region of the outer sheet with a limited range of angle values (between 54° and 90° for S1C15E and between 56° and 76° for S2C15E). During the spanning of the hydrophobic core, the angle can fluctuate more. In the inner sheet, the mass center is located at −15.75 and −15 Å for S1C15E and S2C15E, respectively, when the minimal energy is reached. At this position the fatty acid chain forms an angle of −22° and −45° with the plane of the bilayer for S1C15E and S2C15E, respectively.

The optimal orientations of the C15 homologue (i.e. the position and the orientation at the lowest restraint value) in the two bilayer models (uncharged and charged) are shown in Figures 7 and 8.

In the uncharged membrane, the molecule is completely embedded in the bilayer while in the charged membrane a part of the peptide ring is in the aqueous medium. The location of the acidic residues depends on the ring conformer. In the uncharged membrane, S1 molecules have their aspartic lateral chain in the polar head region while the glutamic residues are in the hydrophobic core of the bilayer. In the charged membrane, the aspartic lateral chain protrudes in the aqueous medium when the glutamic residue remains in the polar head region. For the S2 conformations, the two acid residues are in the polar head region irrespective of the type of membrane. The fatty acid chain is located in the hydrophobic core of the uncharged bilayer and at the hydrophobic core/polar head interface of the inner sheet in the charged membrane. In this case, it presents an oblique orientation when it is extended.

Simulation of Surfactin Assembly. The interaction of surfactin with itself and with phospholipids was studied using HYPERMATRIX.[17] The most common phospholipids in biological membranes were considered: dipalmitoyl phosphatidylcholine (DPPC) and dipalmitoyl phosphatidylethanolamine (DPPE) as neutral phospholipids, and dipalmitoyl phosphatidylserine (DPPS) as a negatively charged phospholipid.

The assembly of surfactin C15 molecules (Figure 9) is a cone-shaped structure. The peptide rings make the large cone basis and the fatty acid chains interact with each other.

The interactions between surfactin molecules are always lower in energy than the interactions between a surfactin molecule and phospholipids, whether the phospholipids are charged or not (Figure 10).

Moreover, for one ring conformer (S1 or S2), the greater the carbon atom number, the more favorable the interaction energy. This is particularly true for the S2 conformer. The S1 conformation does not allow an efficient interaction between fatty acid chains because of steric hindrance.

Hemolytic Activity and Critical Micelle Concentration of Surfactin Homologues. The hemolytic activity was measured on sheep erythrocytes. The hemolysis percentage depends on the concentration (Figure 11).

It is also influenced by the length of the fatty acid chain of surfactin. The longer the chain, the higher the hemolytic activity is. The concentration required to obtain 50% hemolysis is 3-fold lower for the C15 than for the C13 surfactin.

The critical micelle concentrations (cmc's) of the three surfactin homologues (Table 2) are between 19.5 and 83.6 μM, depending on the hydrophobicity of the fatty acid chain.

They are very low as compared to those of classical surfactants such as SDS (cmc = 2.30 mM), Triton X-100 (cmc = 0.3 mM), CTAB (cmc = 1 mM), and CHAPS (cmc = 6−10 mM).[33] The cmc value of the surfactin decreases when the hydrophobicity of the fatty acid chain increases.

Discussion

Previous studies focused on the different mechanisms of surfactin in biological systems, leading to various hypotheses:

(1) Surfactin is a mobile cation carrier.[10]

(2) Surfactin molecules form cationic channels.[9]

(3) Surfactin disrupts the phospholipid organization, leading to membrane destruction by a detergent effect.[37]

In this study, two computational methods were used to compare the different hypotheses in combination with cmc

(36) Black, S. D. http://psyche.uthct.edu/shaun/Sblack/detergnt.html. 2002.

(37) Peypoux, F.; Bonmatin, J. M.; Wallach, J. *Appl. Microbiol. Biotechnol.* **1999**, *51*, 553−563.

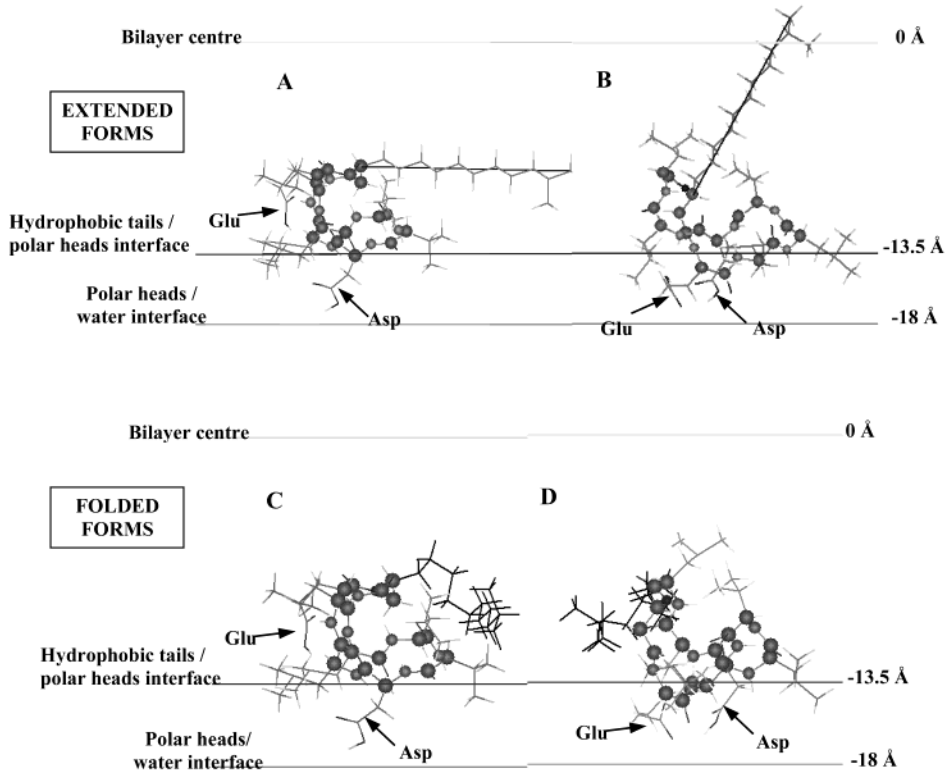

Figure 7. Representation of C15 surfactin in the uncharged membrane corresponding to its position in the bilayer when the total restraint is minimal: A, S1C15E; B, S2C15E; C, S1C15F; D, S2C15F.

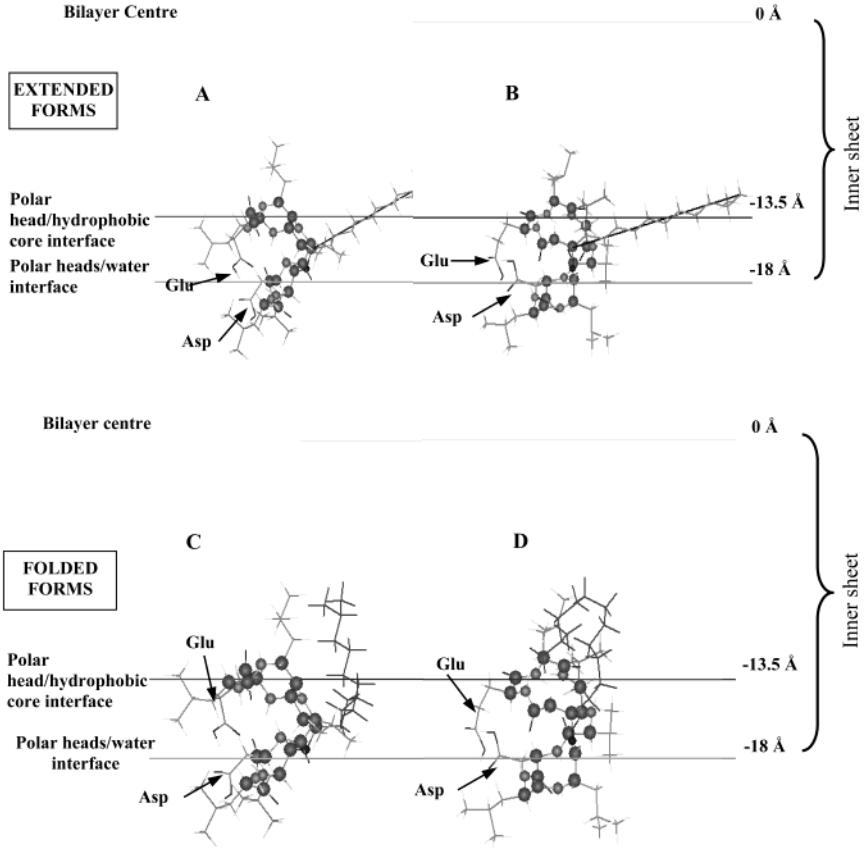

Figure 8. Representation of C15 surfactin in the charged membrane corresponding to its position in the bilayer when the total restraint is minimal: A, S1C15E; B, S2C15E; C, S1C15F; D, S2C15F.

data. This leads to a molecular description of the biological mechanisms of surfactin, more specifically of its hemolytic activity.

Mobile Cation Carrier Hypothesis. According to Thimon et al.,[10] surfactin is a mobile carrier that transports monovalent and divalent cations across a membrane. The

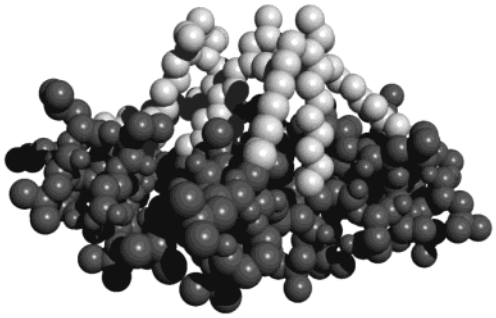

Figure 9. CPK view of the multimolecular assembly of S1C15E: light gray = acyl chains; dark gray = peptide rings.

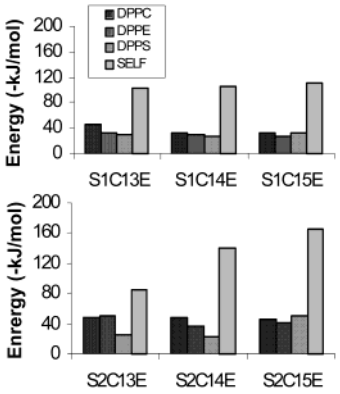

Figure 10. Energies of interaction of the extended surfactin molecule with other surfactin molecules and with different phospholipids: dipalmitoyl phosphatidylcholine (DPPC) and dipalmitoyl phosphatidylethanolamine (DPPE) as neutral phospholipids, and dipalmitoyl phosphatidylserine (DPPS) as a negatively charged phospholipid.

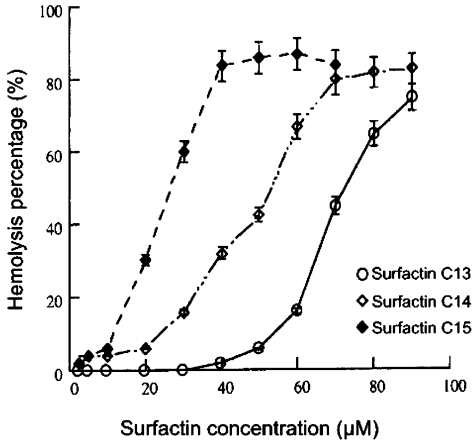

Figure 11. Hemolysis percentage of sheep erythrocytes (suspension of 5×10^8 cells/mL) as a function of the surfactin concentration for the three surfactin homologues.

complexation of cations by interaction with the negative charges of the Asp and Glu residues takes place at the interface, leading to the solubilization of the complex in the lipid phase.

Since a lower total restraint corresponds to a more favorable position, our results suggest that surfactin is preferentially inserted in membrane rather than in water.

For the uncharged bilayer model, the low variation of the total restraint within the bilayer suggests that surfactin is able to cross the membrane both ways. The minimum of energy observed when the surfactin center is in the polar head region is not very different from the energy value when it is in the hydrophobic core, suggesting a low energy barrier for crossing. In the charged membrane, the sharp decrease of the total energy restraint in the inner sheet indicates that surfactin preferentially stands at this place.

Table 2. Critical Micelle Concentration (in μM) of the Three Surfactin Homologues in a Tris-HCl pH 8.0 Buffer at 20.0 °C

surfactin	cmc (μM)
Surfactin C13	83.6
Surfactin C14	65.1
Surfactin C15	19.5

The difference between the energy profiles of the uncharged and the charged models highlights the influence of the membrane composition, and more particularly the negative phospholipids, on the capability of surfactin to transport cations across the membrane, both ways.

In both cases, the molecule flips around when surfactin goes from the outer to the inner sheet, as indicated by the angle sign inversion (Figures 4 and 6).

Hence, the simulations are in agreement with the mobile carrier hypothesis. According to our results, surfactin can penetrate in the outer sheet, with its fatty acid chain interacting with the acyl chains of the phospholipids, as suggested by Maget-Dana and Ptak.[14] Its peptide ring is located near the phospholipid polar heads, which allows the formation of a cation complex. Then, the molecule crosses the bilayer. Its turnaround allows the peptide ring to interact with the phospholipid polar heads of the inner sheet and the cation to be delivered in the intracellular medium. The simulations indicate that this mechanism occurs for all surfactin homologues.

The difference between the total restraints of the S1 and S2 conformers is not sufficient to decide in favor of one of them. A reversible transition between the two conformers could occur during the penetration and the spanning of the surfactin in the bilayer. A similar mechanism has been demonstrated for other ionophores such as ionomycin[38] and lasalocid A.[39] In the simulations with an uncharged membrane, a difference of orientation and position is observed between conformers (S1 and S2). In S1, the Asp and Glu residues are more far apart than they are in S2. It could be suggested that the S2 conformer corresponds to surfactin complexing a calcium ion, while the S1 one corresponds to the molecule being cation free.

Hypothesis of the Ionic Channel Formation. The formation of cationic channels requires molecule association across the bilayer. According to our results, surfactin does not span through the bilayer. It is thus unfavorable to channel formation unless surfactin molecules could self-associate inside the membrane. Successive self-associated structures could then link together to form a channel-like supramolecular structure. This is more likely to occur for an uncharged membrane where there is a minimal energy position in both the outer and the inner leaflets, but not in the charged membrane, where the surfactin is preferentially in the charged leaflet. This explanation is in agreement with the results of Sheppard et al.,[9] who show channel formation in a lipid bilayer constituted by glycerol monooleate, that is, a neutral lipid, when adding surfactin to the aqueous phase on both sides of the membrane.

Hypothesis of the Detergent Effect. The oblique insertion of extended surfactin in the bilayer could explain its detergent effect. Indeed, the lipid perturbation restraint term obtained by decomposition of the total restraint is

(38) Brasseur, R.; Notredame, M.; Ruysschaert, J.-M. *Biochem. Biophys. Res. Commun.* **1983**, *114*, 632−637.
(39) Brasseur, R.; Deleers, M.; Russchaert, J.-M. *Biosci. Rep.* **1984**, *4*, 651−655.

energetically unfavorable. However, its magnitude is not very important as compared to those for the other restraints (data not shown).

The insertion of a single surfactin molecule does not highly disorganize the phospholipids. It could, however, be the first step of the membrane solubilization by a detergent effect. Indeed, according to Lasch and Kragh-Hansen et al.'s observations[40,41] on other surfactants, membrane solubilization is preceded by a detergent partition into the membrane phase.

The energies calculated with HYPERMATRIX show that surfactin molecules prefer to self-associate rather than to associate with lipids. The cone-shape complex of surfactin could explain its ability to form micelles. This supports the hypothesis that, after the insertion of several molecules of surfactin in the membrane, mixed micelles of surfactin and phospholipids could lead to the bilayer solubilization. It is in accordance with the second step of the detergent effect described by Lasch and Kragh-Hansen et al.[40,41]

The hypothesis of preferential surfactin−surfactin interactions in a membrane has already been suggested by Deleu et al.,[42,43] who observed surfactin domain formation in a dipalmitoyl phosphatidylcholine monolayer. Grau et al.[44] have also observed that surfactin clusters with phospholipids. Clusters are segregated as domains within the bilayer. The detergent effect of surfactin has also been suggested by Heerklotz and Seelig.[11]

According to the model and the cmc measurements, the self-association of surfactin is influenced by the fatty acid chain hydrophobicity. The second step of the detergent effect would vary with the surfactin homologue, with C15 being the most active.

Mechanism Involved in Hemolytic Activity. The hemolytic activity of surfactin on sheep erythrocytes depends on the fatty acid chain hydrophobicity, in accordance with the results of Kracht et al.[15] on human erythrocytes.

This effect is not obvious in the IMPALA simulation that considers an isolated surfactin molecule, even if the bilayer charge distribution is that of an erythrocyte membrane. However, the energies obtained by HYPERMATRIX show an influence of the fatty acid chain hydrophobicity on the self-association capacity of surfactin, as observed for the hemolytic activity and the cmc.

Accordingly, we propose that the hemolytic activity is related to the surfactin association capacity, and thereby to the detergent mechanism for which the second step was suggested to depend on this factor. The relationship between the biological activity and the association state has also been suggested for another lipopeptide, iturin A.[45]

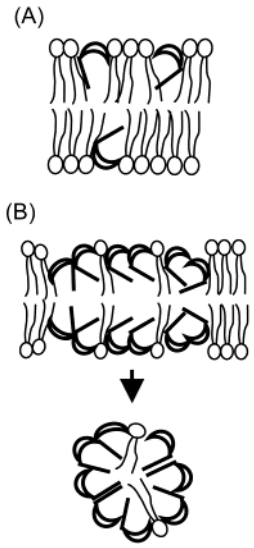

Figure 12. Schematic representation of the detergent effect of surfactins in two steps: (A) at low concentration, penetration of the surfactin in the bilayer; (B) at concentrations closer to the cmc, formation of micelles including membrane phospholipids, leading to the solubilization of the bilayer.

Conclusion

IMPALA simulations have shown that surfactin penetrates into charged and uncharged bilayers. The difference between the three surfactin homologues is negligible. However, the energies of interaction obtained by HYPERMATRIX have shown a dependence of the surfactin self-association on its chain hydrophobicity.

On the basis of these simulations and cmc data, we suggest that the hemolytic activity of surfactin results from the erythrocyte membrane destruction by the detergent effect, which depends on the surfactin concentration as illustrated in Figure 12.

In the first step, a low concentration of surfactin penetrates into the erythrocyte membrane by interacting via its fatty acid chain. In a second step, approaching the cmc, surfactin molecules self-associate to form micelles involving membrane phospholipids and leading to membrane rupture. The self-association capacity (as shown with HYPERMATRIX and cmc measurements) depends on the fatty acid chain hydrophobicity and could be involved in the antiviral activity.

Our results emphasize the influence of the membrane composition on the surfactin activity. The mechanism is different depending on the nature of the membrane and the surfactin concentration. Several mechanisms can also occur simultaneously. The hypothesis of the cationic channels formation and of the mobile carrier cannot be ruled out.

Acknowledgment. R.B. and M.D. thank the FNRS (Belgium) for their positions as Director of Research and Research Assistant, respectively. O.B. is supported by the "Ministère de la Région wallonne (Direction Générale des Technologies, de la Recherche et de l'Energie)", grant #14540. This work received support from the FNRS via a FRFC project (#2.4558.98). The authors thank Prof. Annick Thomas and Dr. Ho Bosco for their critical reading.

LA026543Z

(40) Lasch, J. *Biochim. Biophys. Acta* **1995**, *1241*, 269−292.
(41) Kragh-Hansen, U.; Le Maire, M.; Moller, J. V. *Biophys. J.* **1998**, *75*, 2932−2946.
(42) Deleu, M.; Paquot, M.; Jacques, P.; Thonart, P.; Adriaensen, Y.; Dufrêne, Y. F. *Biophys. J.* **1999**, *77*, 2304−2310.
(43) Deleu, M.; Nott, K.; Brasseur, R.; Jacques, P.; Thonart, P.; Dufrêne, Y. F. *Biochim. Biophys. Acta* **2001**, *1513*, 55−62.
(44) Grau, A.; Fernández, J. C. G.; Peypoux, F.; Ortiz, A. *Biochim. Biophys. Acta* **1999**, *1418*, 307−319.
(45) Harnois, I.; Genest, D.; Brochon, J. C.; Ptak, M. *Biopolymers* **1988**, *27*, 1403−1413.